arXiv:0710.3310v1 [cond-mat.soft] 17 Oct 2007

Two-parameter model predictions and θ-point crossover for linear-polymer solutions

Sergio Caracciolo
Dipartimento di Fisica, Università degli Studi di Milano,
and INFN – Sezione di Milano I
Via Celoria 16, I-20133 Milano, Italy
e-mail: `Sergio.Caracciolo@mi.infn.it`

Bortolo Matteo Mognetti
Institut für Physik, Johannes Gutenberg-Universität,
Staudinger Weg 7, D-55099 Mainz, Germany
e-mail: `mognetti@uni-mainz.de`

Andrea Pelissetto
Dipartimento di Fisica,
Università degli Studi di Roma "La Sapienza"
and INFN – Sezione di Roma I
P.le A. Moro 2, I-00185 Roma, Italy
e-mail: `Andrea.Pelissetto@roma1.infn.it`

We consider the first few virial coefficients of the osmotic pressure, the radius of gyration, the hydrodynamic radius, and the end-to-end distance for a monodisperse polymer solution. We determine the corresponding two-parameter model functions which parametrize the crossover between the good-solvent and the ideal-chain behavior. These results allow us to predict the osmotic pressure and the polymer size in the dilute regime in a large temperature region above the θ point.

PACS: 61.25.Hq, 82.35.Lr

I. INTRODUCTION

Polymeric fluids exhibit a rich and complex set of phenomena associated both with system-specific and global properties of the polymer molecules. Chemical details become increasingly less relevant for global polymer properties as the degree of polymerization N increases.[1,2,3,4,5] Thus, for $N \to \infty$, one can use coarse-grained models in which only the most fundamental aspects of the polymer structure are taken into account. The behavior of polymer solutions depends in general on temperature. For T large enough, the most relevant feature is the local repulsion. In this regime, usually called *good-solvent* regime, the radius of gyration R_g, as well as any other quantity that is related to the global size of the polymer, scales as N^ν, where ν is a universal exponent; $\nu \approx 0.5876$ (Ref.[6]). As T is lowered, one reaches the θ temperature, T_θ, below which polymers are compact ($R_g \sim N^{1/3}$) and phase separation occurs.[7] At the θ point polymers behave approximately as Gaussian coils. The crossover from good-solvent to θ behavior is well understood. For $N \to \infty$ any global quantity $\mathcal{O}$ behaves as:[5,8]

$$\mathcal{O}(T, N, c) = \alpha_1 \mathcal{O}_G(N, c) f_{\mathcal{O}}[\alpha_2 (T - T_\theta) N^{1/2} (\ln N)^{-4/11}, \alpha_3 c \hat{R}_g^3(T, N)]. \tag{1.1}$$

Here c is the polymer number density, $\hat{R}_g(T, N)$ is the zero-density radius of gyration, and $\mathcal{O}_G(N, c)$ is the expression of $\mathcal{O}$ for ideal chains. The function $f_{\mathcal{O}}(x, y)$ is universal, all chemical details being included in the constants α_i.

Eq. (1.1) is strictly valid only for $N \to \infty$, $T \to T_\theta$, at fixed $\alpha_2(T - T_\theta) N^{1/2} (\ln N)^{-4/11}$. For finite values of N one should also take into account the corrections to Eq. (1.1) that decay very slowly, as inverse powers of $\ln N$. In Ref.[9] we computed the crossover curve for the interpenetration ratio Ψ and found that logarithmic corrections are only relevant very close to T_θ. Outside a *tricritical region* around T_θ, Eq. (1.1) provides a reasonably accurate description of the crossover. As emphasized in Ref.[10], in order to compute the crossover functions defined in Eq. (1.1) one can use the continuum two-parameter model (TPM).[11] Indeed, if we identify $(T - T_\theta) N^{1/2} (\ln N)^{-4/11}$ with the Zimm-Stockmayer-Fixman[12] variable z (with a model-dependent proportionality factor), then the crossover function for $\mathcal{O}$ corresponds exactly to its TPM expression.

It is interesting to note that the TPM is also of interest to describe the corrections to scaling in some polymeric systems. Indeed, as discussed in Ref.[13], the TPM describes the approach to the scaling limit when $V_m / l^3 \ll 1$, where l is the persistence length and V_m is the volume occupied by a polymer blob of length l.

In this paper we wish to compute the crossover functions for several quantities whose behavior in the good-solvent regime has been considered in Refs.[14,15]. We compute numerically the TPM predictions for the second, third, and fourth virial coefficient, for the swelling factors, and the density corrections to the radius of gyration, the end-to-end distance, and the hydrodynamic radius. This allows us to give exact predictions for the thermodynamic behavior and for the polymer size in the whole dilute regime $\Phi_p \lesssim 1$, where Φ_p is the polymer volume fraction.

The paper is organized as follows. In Sec. II we define the TPM as the scaling limit of the lattice Domb-Joyce model. This is a rigorous well-defined definition that does not rely on perturbative field theory. In Sec. III we define the quantities that are considered in the paper and report some results and properties that are useful in the following section. In Sec. IV we give the results of our work. We first report the analysis of the Monte Carlo results and then determine the TPM functions associated with the different quantities. In Sec. IV C and IV D we use these results to predict the osmotic pressure and the polymer size in the dilute and in the semidilute regime. Finally, in Sec. IV E we compare our predictions with the available renormalization-group results. Some conclusions are presented in Sec. V.

II. THE DOMB-JOYCE MODEL

In order to compute the TPM crossover functions, we consider the three-dimensional lattice Domb-Joyce (DJ) model.[16] We consider a cubic lattice and model a polymer of length N as a random walk $\{\mathbf{r}_0, \mathbf{r}_1, \ldots, \mathbf{r}_N\}$ with $|\mathbf{r}_\alpha - \mathbf{r}_{\alpha+1}| = 1$ on a cubic lattice. To each walk we associate a Boltzmann factor

$$e^{-\beta H} = e^{-w\sigma}, \qquad \sigma = \sum_{0 \le \alpha < \beta \le N} \delta_{\mathbf{r}_\alpha, \mathbf{r}_\beta}, \tag{2.1}$$

with $w > 0$. The factor σ counts how many self-intersections are present in the walk. This model is similar to the standard self-avoiding walk (SAW) model, in which polymers are modelled by random walks in which self-intersections are forbidden. The SAW model is obtained for $w = +\infty$. For finite positive w self-intersections are possible although energetically penalized. For any positive w, this model has the same scaling limit of the SAW model[16] and thus allows us to compute the universal scaling functions that are relevant for polymer solutions.

The DJ model can be efficiently simulated by using the pivot algorithm.[17,18,19,20] For the SAW an efficient implementation is discussed in Ref.[21]. The extension to the DJ model is straightforward, the changes in energy being taken into account by means of a Metropolis test. Such a step should be included carefully in order not to loose the good scaling behavior of the CPU time for attempted move. We use here the implementation discussed in Ref.[22].

The TPM results can be derived from simulations of the DJ model. Indeed, the continuum results are obtained[23] by taking the limit $w \to 0$, $N \to \infty$ at fixed product $wN^{1/2}$ (we call it x). The variable x interpolates between the ideal-chain limit ($x = 0$) and the good-solvent limit ($x = \infty$). Indeed, for $w = 0$ the DJ model is simply the random-walk model, while for any $w \neq 0$ and $N \to \infty$ one always obtains the good-solvent scaling behavior. The variable x is directly related to the variable z that is usually used in the TPM context:[23] indeed, $z = \alpha x$. The normalization factor α can be fixed by considering the small-z behavior of the interpenetration ratio Ψ: conventionally one takes $\Psi = z + O(z^2)$. In the DJ model[24] $\Psi \equiv (3/2\pi)^{3/2} wN^{1/2}$ for small $wN^{1/2}$, so that we can identify

$$z = \left(\frac{3}{2\pi}\right)^{3/2} wN^{1/2}. \tag{2.2}$$

III. DEFINITIONS

We consider the osmotic pressure $\Pi(T, N, c)$ or, equivalently, the adimensional compressibility factor

$$Z(T, N, c) \equiv \frac{M\Pi}{RT\rho} = \frac{\Pi}{k_B T c}, \tag{3.1}$$

where c is the polymer number density, ρ the weight concentration, M the molar mass of the polymer, T the absolute temperature, k_B and R the Boltzmann and the ideal-gas constants. In the dilute limit, Z can be expanded in powers of the concentration as

$$Z = 1 + \sum_{n \geq 2} A_n (c\hat{R}_g^3)^{n-1}, \tag{3.2}$$

where $\hat{R}_g$ the zero-density radius of gyration. The coefficients A_n depend on T, N, and on chemical details. However, in the good-solvent regime, they converge to universal constants A_n^* as $N \to \infty$. Moreover, the renormalization group predicts that corrections should always scale as $N^{-\Delta}$, where Δ is a universal exponent whose best estimate is[24] $\Delta = 0.515 \pm 0.007^{+0.010}_{-0.000}$. Therefore, for large N we expect

$$A_n(T, N) = A_n^* + A_{1,n}(T) N^{-\Delta} + \cdots \tag{3.3}$$

While the constants A_n^* are universal, the coefficients $A_{1,n}(T)$ are system specific and temperature dependent. However, the ratios

$$b_n \equiv \frac{A_{1,n}(T)}{A_{1,2}(T)} \tag{3.4}$$

are also universal. Precise estimates of A_n for $n \leq 4$ and of b_3 have been obtained in Ref.[14]:

$$A_2^* = 5.500 \pm 0.003, \tag{3.5}$$

$$A_3^* = 9.80 \pm 0.02, \tag{3.6}$$

$$A_4^* = -9.0 \pm 0.5, \tag{3.7}$$

$$b_3 = 4.75 \pm 0.30. \tag{3.8}$$

Instead of A_2 it is customary to define the interpenetration ratio[25] $\Psi \equiv 2(4\pi)^{-3/2} A_2$, whose large-$N$ value in the good-solvent regime is[14] $\Psi^* = 0.24693 \pm 0.00013$ (Ref.[14]), $\Psi^* = 0.24685 \pm 0.00011$ (Ref.[26]).

In the TPM, the coefficients A_n become functions of z, $A_n(z)$, such that $A_n(z=0)=0$ ($z=0$ is the ideal-chain case) and $A_n(z=\infty)=A_n^*$. Since $z \sim N^{1/2}$, Eq. (3.3) implies

$$A_n(z) = A_n^* + a_n z^{-2\Delta} \tag{3.9}$$

for large z, with $a_n/a_2 = b_n$.[27]

The small-z behavior of the TPM functions can be determined by using perturbation theory.[4,11] We quote here the result for $A_2(z)$ and $A_3(z)$:[28,29,30]

$$\begin{aligned} A_2(z) &= \frac{1}{2}(4\pi)^{3/2} z[1 - 4.779663z + 25.58964z^2 + O(z^3)], & (3.10)\\ A_3(z) &= \frac{2}{35}\left(\frac{16\pi}{3}\right)^3 (208\sqrt{2} - 108\sqrt{3} - 103)z^3 + O(z^4) \approx 1100.7z^3. & (3.11) \end{aligned}$$

In the appendix we compute the leading contribution to $A_4(z)$ obtaining

$$A_4(z) = \frac{131072}{45045}(14075 + 12624\sqrt{2} - 18468\sqrt{3})\pi^{9/2} z^4 + O(z^5) \approx -29883.1z^4. \tag{3.12}$$

Beside the osmotic pressure we consider three different quantities that characterize the polymer size: the radius of gyration R_g, the hydrodynamic radius R_H, and the end-to-end distance. In the DJ lattice model they are defined as follows:

$$\begin{aligned} R_g^2 &\equiv \frac{1}{2(N+1)^2}\left\langle \sum_{\alpha\beta} (\mathbf{r}_\alpha - \mathbf{r}_\beta)^2 \right\rangle, & (3.13)\\ \frac{1}{R_H} &\equiv \frac{1}{(N+1)^2}\left\langle \sum_{\alpha\beta:\mathbf{r}_\alpha \neq \mathbf{r}_\beta} \frac{1}{|\mathbf{r}_\alpha - \mathbf{r}_\beta|} \right\rangle, & (3.14)\\ R_e^2 &\equiv \langle (\mathbf{r}_0 - \mathbf{r}_N)^2 \rangle . & (3.15) \end{aligned}$$

We also define the ratios

$$A_{ge} \equiv \frac{\hat{R}_g^2}{\hat{R}_e^2} \qquad\qquad A_{gH} \equiv \frac{\hat{R}_g}{\hat{R}_H}, \tag{3.16}$$

where a hat indicates a zero-density quantity, and consider the density expansions

$$\begin{aligned} \frac{R_g^2}{\hat{R}_g^2} &= 1 + S_{1,g}(c\hat{R}_g^3) + S_{2,g}(c\hat{R}_g^3)^2 + \cdots \\ \frac{R_e^2}{\hat{R}_e^2} &= 1 + S_{1,e}(c\hat{R}_g^3) + S_{2,e}(c\hat{R}_g^3)^2 + \cdots \\ \frac{\hat{R}_H}{R_H} &= 1 + S_{1,H}(c\hat{R}_g^3) + S_{2,H}(c\hat{R}_g^3)^2 + \cdots & (3.17) \end{aligned}$$

The ratios (3.16) and the density coefficient $S_{n,\#}$ are system-dependent quantities. However, as $N \to \infty$ in the good-solvent limit, they approach universal quantities, which will be labelled as A_{ge}^*, A_{gH}^*, and $S_{n,\#}^*$. The limiting values of the ratios and of the density coefficients for $n = 1, 2$ have been determined in Ref.[15].

In the TPM all previous quantities are functions of z which converge to their good-solvent value for $z \to \infty$. If Q corresponds to A_{ge} or to a coefficient S_n for the radius of gyration and the end-to-end distance, we can also determine the corrections for $z \to \infty$. Indeed, in this limit, we have

$$Q = Q^* + a_Q z^{-2\Delta}. \tag{3.18}$$

The ratio a_Q/a_2 [a_2 is defined in Eq. (3.9)] is universal; estimates for A_{ge}, $S_{1,g}$, and $S_{1,e}$ are reported in Ref.[15]. For $z \to 0$, $S_{n,\#}(z=0)=0$, while A_{ge} and A_{gH} converge to the ideal-chain (random-walk) values

$$A_{ge}(z=0) = \frac{1}{6} \qquad\qquad A_{gH}(z=0) = \frac{8}{3\sqrt{\pi}}. \tag{3.19}$$

The leading corrections for $z \to 0$ to all these quantities are reported in the Appendix.

Finally, we consider the swelling factors for the zero-density radii:

$$\hat{R}_g^2 = \frac{1}{6} N \ell^2 \alpha_g^2(z), \tag{3.20}$$

$$\hat{R}_e^2 = N \ell^2 \alpha_e^2(z), \tag{3.21}$$

$$\hat{R}_H = \frac{1}{8} \left(\frac{3\pi}{2}\right)^{1/2} \sqrt{N} \ell \alpha_H(z) \ . \tag{3.22}$$

The swelling factors are normalized so that $\alpha_\#(z = 0) = 1$. In the DJ model the metrical factor ℓ is equal to the lattice spacing. For $z \to \infty$ they behave as

$$\alpha_\# = \alpha_{0,\#} z^{2\nu-1}(1 + \alpha_{1,\#} z^{-2\Delta} + \cdots) \tag{3.23}$$

For the hydrodynamic radius one should additionally consider corrections proportional[31] to $z^{4\nu-4}$.

IV. CROSSOVER FUNCTIONS

A. Monte Carlo results

The main purpose of the present paper is the determination of the crossover functions for the quantities defined in Sec. III. We consider five different values of z, which we denote by z_1, ..., z_5, which belong to the crossover region between ideal and good-solvent behavior. Explicitly we use $z_1 = 0.056215$, $z_2 = 0.148726$, $z_3 = 0.32165$, $z_4 = 0.728877$, and $z_5 = 2.50828$. They were chosen so that $A_2(z_n) \approx n$ (remember that $A_2(z)$ varies between 0 and 5.50). In order to compute the TPM value for each z_i, we perform several simulations at values (w_{ij}, N_{ij}) such that $w_{ij} N_{ij}^{1/2} = (2\pi/3)^{3/2} z_i$, choosing N_{ij} between 100 and 8000. Then, we fit each universal quantity Q with the theoretically expected behavior:[23,24,32]

$$Q(w_{ij}, N_{ij}) = Q^*(z_i) + N_{ij}^{-1/2} b_Q(z_i) + N_{ij}^{-1} c_Q(z_i). \tag{4.1}$$

The TPM result corresponds to the leading term $Q^*(z_i)$. In order to detect additional scaling corrections that are not taken into account by the fit ansatz (4.1), we have repeated the fit several times, each time including only data satisfying $N \geq N_{\min}$.

We illustrate the procedure by considering A_2. In Fig. 1 we plot $A_2(w, N)$ vs $N^{-1/2}$; for each z we also plot the function $Q^* + N^{-1/2} b_Q$ obtained in the fit of all data ($N_{\min} = 100$) to Eq. (4.1). The data points follow the expected behavior quite precisely, with very small N^{-1} corrections. Note that an extrapolation is always needed except for very small values of z. Estimates of $A_2(z)$ are reported in Table I for different values of $N_{\min}$. No systematic deviations are observed. We take the results corresponding to $N_{\min} = 500$ as our final results. They are reported in Table II. We have applied the same analysis to A_3, A_4, A_{ge}, A_{gH}, $S_{n,g}$, $S_{n,e}$, $S_{n,H}$ $(n = 1, 2)$. The results corresponding to $N_{\min} = 500$ are reported in Table II.

Finally, we determine the swelling factors. We consider $6\hat{R}_g^2/N$, $\hat{R}_e^2/N$, and $k_H\sqrt{N}/\hat{R}_H$ ($k_H = 2^{-7/2}(3\pi)^{1/2}$). The corresponding quantities are reported in Fig. 2. Their behavior with N at fixed z is perfectly consistent with Eq. (4.1). Therefore, we have performed the same fits as before. The results are reported in Table II.

B. Interpolation formulas

We now use the results of Sec. IV A, the good-solvent results of Refs.[14,15], and the small-z results mentioned in Sec. III and in the Appendix, to obtain interpolation formulas that are valid for all values of z. We discuss in detail the virial coefficients; all other quantities are analyzed analogously.

For the second virial coefficient we wish to find an interpolation that satisfies the following properties: (i) for $z \to \infty$ it must satisfy $A_2(z) \to A_2^* = 5.500$ [Eq. (3.5)]; (ii) for $z \to 0$ it must behave as $4\pi^{3/2} z(1 - 4.779663z)$ [Eq. (3.10)]; (iii) the interpolating curve should assume the values determined numerically and reported in

Table II. Since the results for $A_2(z)$ indicate that this function is monotonic, we take an interpolating function of the form

$$A_2(z) = 4\pi^{3/2} z(1 + d_1 z + d_2 z^2 + d_3 z^3 + d_4 z^4)^{-1/4}, \tag{4.2}$$

where d_i are constants to be determined. The constant d_1 can be fixed to obtain the expansion (3.10) to order z^2: we obtain $d_1 = 19.1187$. The constant d_4 can be fixed by requiring $A_2(z = \infty) = A_2^*$, where A_2^* is given in Eq. (3.5): this gives $d_4 = 268.96$. Then, we fit

$$\left[\frac{4\pi^{3/2} z}{A_2(z)}\right]^4 - 1 - d_1 z - d_4 z^4 = d_2 z^2 + d_3 z^3 \ . \tag{4.3}$$

Using the five data reported in Table II we obtain $d_2 = 126.783$ and $d_3 = 331.99$. The interpolation formula is reported in Table III. For $z \to \infty$, Eq. (4.2) gives

$$A_2(z) = 5.500 - 1.6972/z + O(z^{-2}) \ . \tag{4.4}$$

This expression is compatible with Eq. (3.9), taking into account that[24] $2\Delta \approx 1.03$. It allows us to estimate a_2: $a_2 \approx -1.7$. Of course, this is a very rough estimate. A careful determination would require $A_2(z)$ for much larger values of z and a careful analysis of the corrections to the behavior (3.9). Expression (4.4) agrees with the field-theoretical result reported in Ref.[29], which predicts $a_2 \approx 5.50 \times (-0.30) \approx -1.65$.

We now compare the interpolation formula (4.2) with similar expressions that appear in the literature. We consider the expression reported in Ref.[5] (Sec. 15.5.2):

$$A_2(z) = \frac{1}{2}(4\pi)^{3/2} \frac{0.182\tilde{z}(1 + 2.15\tilde{z} + 0.82\tilde{z}^2)^{-0.236}}{(1 + 1.32\tilde{z} + 0.378\tilde{z}^2)^{0.264}}, \tag{4.5}$$

where[33] $z = 0.182\tilde{z}$. Equation (4.5) has been obtained by using a sophisticated form of renormalized one-loop perturbation theory. By means of an extensive Monte Carlo simulation Ref.[24] obtained

$$A_2(z) = \frac{1}{2}(4\pi)^{3/2} z(1 + 14.339z + 60.30z^2 + 66.3z^3)^{-1/3}. \tag{4.6}$$

Finally, we quote the field-theoretical expression of Ref.[34] for $\epsilon = 1$:

$$A_2(z) = \frac{1}{2}(4\pi)^{3/2} \left\{ \frac{\eta}{8(1+\eta)} + \frac{1}{64}\left[\left(4\ln 2 + \frac{7}{6}\right)\left(\frac{\eta}{1+\eta}\right)^2 + \frac{21\eta}{4(1+\eta)}\right]\right\}, \tag{4.7}$$

with $\eta = 256z/53$ (this relation is obtained by matching the small-z behavior). Our result (4.2) is essentially identical to Eq. (4.6): differences are less than 0.3%. It is also in very good agreement with the field-theoretical result (4.5), differences being less than 1.5%. Eq. (4.7) is worse: the difference is of order 8% for $z = 0.1$ and increases to 12% for large values of z.

Let us now discuss A_3. We will use an interpolation formula analogous to (4.2), setting

$$A_3(z) = 1100.7z^3(1 + d_1 z + d_2 z^2 + d_3 z^3 + d_4 z^4)^{-3/4}. \tag{4.8}$$

The prefactor has been fixed by using Eq. (3.11). To determine the coefficients we use a strategy slightly different from that discussed for A_2, since we only know the leading small-z behavior of A_3 and thus we cannot fix d_1 by using perturbation theory. Instead, we make use of the results of Ref.[14] to obtain the large-z behavior of $A_3(z)$. Since[14] $b_3 = a_3/a_2 = 4.75$ [see Eq. (3.9)], Eqs. (4.4) and (3.6) give $A_3(z) \approx 9.80 - 8.062/z$ (again we use the approximation $2\Delta \approx 1$). If we require Eq. (4.2) to reproduce this expansion, we obtain $d_3 = 594.386$ and $d_4 = 541.906$. Finally, we fit the results of Table II to determine d_1 and d_2. The resulting expression is reported in Table III.

Finally, we consider A_4. In this case we do not know a_4/a_2 and thus we use an interpolation formula with only three parameters:

$$A_4(z) = -29883.1z^4(1 + d_1 z + d_2 z^2 + d_3 z^3)^{-4/3}. \tag{4.9}$$

The prefactor has been fixed by using Eq. (3.12). The constant d_3 is fixed by using Eq. (3.7), d_1 and d_2 by fitting the numerical results of Table II. The final expression is reported in Table III. In Fig. 3 we report the crossover functions for A_2, A_3, A_4. They are monotonic and approach the good-solvent value for $z \gtrsim 5$.

Similar analyses are performed for the density corrections to the radii. In this case, however, the crossover functions are not monotonic. For the second density correction, this is evident from the numerical data. For instance, $S_{2,g}$ and $S_{2,e}$ are first positive and increasing, in agreement with Eqs. (A12), (A17), reach a maximum for $0.5 \lesssim z \lesssim 1$, and then decrease, converging to the good-solvent value which is negative. The density coefficient $S_{2,H}$ behaves in the opposite way, but note that, because of its definition, $S_{2,H}$ is equivalent in some sense to $-S_{2,e}$ and $-S_{2,g}$. For the first density correction the nonmonotonicity can be inferred by using the results of Ref.[15]. If $S_{1,\#} = S^*_{1,\#}(1 + \lambda_\# z^{-2\Delta})$, we have $\lambda_\# A^*_2/a_2 \approx -0.050$ for both $S_{1,e}$ and $S_{1,g}$ [a_2 is defined in Eq. (3.9)]. Using $a_2 \approx -1.697$ [Eq. (4.4)], we obtain:

$$S_{1,g} \approx -0.3152 - 0.0049/z^{2\Delta}, \qquad S_{1,e} \approx -0.3853 - 0.0059/z^{2\Delta}. \tag{4.10}$$

Thus, the first density correction vanishes for $z = 0$, then decreases, becomes smaller than the good-solvent value, and eventually converges to it from below. This effect is however numerically very small and thus the nonmonotonic approach is in practice irrelevant. The nonmonotonic behavior requires interpolation formulas slightly different from those used for the virial coefficients. For instance, expressions like (4.2) cannot change sign and thus are unsuitable for $S_{2,\#}$. Our interpolations are reported in Table III and plotted in Fig. 4. Note that the interpolations of $S_{2,\#}$ are not very precise in the region $0.5 \lesssim z \lesssim 1$, since here the functions change their behavior and we do not have enough data points to identify precisely where the functions reach their maximum.

Finally, let us consider the swelling factors. Because of Eq. (3.23), we use an interpolation of the form

$$\alpha_\# = (1 + b_1 z + b_2 z^2 + b_3 z^3)^{(2\nu-1)/3}, \tag{4.11}$$

taking[24] $\nu = 0.58758$. The coefficient b_1 is fixed by requiring $\alpha_\#$ to reproduce the small-z behavior reported in the appendix, while b_2 and b_3 are obtained by interpolating the numerical data. The results are reported in Table III and shown in Fig. 5. Note that α_e, α_g, α_H behave in a very similar way, differences being tiny. For α_g we also show the prediction of Ref.[24], $\alpha_g = (1 + 7.286z + 9.51z^2)^{0.087583}$, and that of Ref.[5], $\alpha_g = (1 + 1.32\tilde{z} + 0.378\tilde{z}^2)^{0.088}$, where[33] $z = 0.182\tilde{z}$. The result of Ref.[24] is perfectly consistent with ours. The field-theoretical result [note that in Fig. 5 it can hardly be distinguished from our result for $\alpha_e(z)$] is slightly larger (1% at $z = 5$): differences are mainly related to the different choice of the exponent ν. Finally, for the end-to-end distance we mention the result of Ref.[24]: $\alpha_e = (1 + 7.6118z + 12.05135z^2)^{0.087583}$. Again, this expression is in perfect agreement with ours.

C. The osmotic pressure

Knowledge of the crossover functions for the lowest virial coefficients provides the osmotic pressure in the dilute regime in which $\Phi_p \lesssim 1$, where Φ_p is the polymer packing fraction,

$$\Phi_p \equiv \frac{4\pi \hat{R}_g^3}{3} c = \frac{4\pi \hat{R}_g^3}{3} \frac{N_A}{M} \rho, \tag{4.12}$$

N_A the Avogadro number, M the molar mass of the polymer, c and ρ the number density and the weight concentration, respectively. In Fig. 6 we report the compressibility factor Z defined in Eq. (3.2) for several values of z for $\Phi_p \lesssim 1$. In this range of concentrations the virial expansion converges quite well[14] and thus our interpolations provide accurate estimates of Z as a function of z and Φ_p.

In Ref.[14] it was shown that a resummation of the virial expansion by using the known large-Φ_p behavior provides a reasonably accurate expression for Z valid in the whole semidilute region. Here we apply the same method to the determination of the leading $z^{-2\Delta}$ correction to the good-solvent value. Since $A_n = A^*_n + a_n z^{-2\Delta}$ for large z, we can write

$$Z(z, N, c) \approx Z^*(N, c) + z^{-2\Delta} Z_1(N, c)\ . \tag{4.13}$$

The functions $Z^*(N, c)$ and $Z_1(N, c)$ depend on c and N. However, for $N \to \infty$, the renormalization group predicts that they become universal functions of the packing fraction Φ_p, so that

$$Z(z, N, c) \approx Z^*(\Phi_p) + z^{-2\Delta} Z_1(\Phi_p). \tag{4.14}$$

The good-solvent function $Z^*(\Phi_p)$ is reported in Ref.[14]. We will now determine the function $Z_1(\Phi_p)$. For this purpose we determine its large-Φ_p behavior. We expect

$$Z_1(\Phi_p) \sim \Phi_p^\alpha, \qquad\qquad \Phi_p \to \infty. \tag{4.15}$$

To fix α, we note that Π is a function of the monomer concentration $c_m \equiv cN$ but not of the degree of polymerization N for $c \to \infty$ (and therefore also $c_m \to \infty$). Hence, $cz^{-2\Delta}\Phi_p^\alpha$ should be independent of N, once c has been replaced by c_m. This condition implies

$$\alpha = \frac{\Delta + 1}{3\nu - 1}. \tag{4.16}$$

In order to understand the region in the (c, z) plane in which expansion (4.14) is valid, we must discuss the expected scaling behavior in the large-concentration limit for generic values of z. In the TPM the osmotic pressure satisfies the general scaling behavior[5]

$$\frac{\Pi}{k_B T} = c\mathcal{P}(c\ell^3 N^{3/2}, z). \tag{4.17}$$

In the limit $z \to 0$ the Flory-Huggins theory applies: for large values of c, Π is proportional to the square of the monomer concentration c_m and to the interaction strength w, so that

$$\frac{\Pi}{k_B T} \sim w c_m^2 \ell^3 \sim cz(c\ell^3 N^{3/2}). \tag{4.18}$$

For large c, the dependence on N should disappear at fixed c_m and w, so that the relevant scaling variable is $z/(c\ell^3 N^{3/2}) = w/(c_m \ell^3)$. Therefore, we obtain the scaling behavior

$$\frac{\Pi}{k_B T} = zc^2\ell^3 N^{3/2} f_Z\left(\frac{z}{c\ell^3 N^{3/2}}\right), \qquad\qquad Z = zc\ell^3 N^{3/2} f_Z\left(\frac{z}{c\ell^3 N^{3/2}}\right). \tag{4.19}$$

The function $f_Z(x)$ is finite for $x \to 0$, while for $x \to \infty$, consistency with (4.14) implies

$$f_Z(x) \approx a_f x^{(3\nu-2)/(3\nu-1)}(1 + b_f x^{-\Delta/(3\nu-1)}). \tag{4.20}$$

The value $f_Z(0)$ can be determined by noting that for $z \to 0$ we can write

$$Z \approx zc\ell^3 N^{3/2} f_Z(0) = A_2 c\hat{R}_g^3 = 4\pi^{3/2} zc(N/6)^{3/2}\ell^3. \tag{4.21}$$

This implies $f_Z(0) = (2\pi/3)^{3/2}/2$.

Eq. (4.19) indicates that, at fixed large z, the compressibility factor shows two different behaviors. If Φ_p is large but still $z \gg c\ell^3 N^{3/2}$, Z increases following Eq. (4.14). If the concentration is further increased, the argument of $f_Z(x)$ decreases and eventually $Z \approx zc\ell^3 N^{3/2} f_Z(0) = 3\sqrt{\pi} z \alpha_g^{-3}\Phi_p$, i.e. Z becomes linear in the concentration. It is clear that this second regime cannot be obtained from extrapolations of results in the dilute region. We will thus consider only concentrations such that $z \gg c\ell^3 N^{3/2}$, so that we can use Eq. (4.14).

To determine the osmotic pressure for densities in the semidilute regime satisfying $z \gg c\ell^3 N^{3/2}$ we expand $A_n(z) = A_n^* + A_{n,1}/z$ for $z \to \infty$. Thus, we obtain for $z \to \infty$

$$\begin{aligned} Z &\approx 1 + 1.31303\Phi_p + 0.558533\Phi_p^2 - 0.122455\Phi^3 \\ &+ \frac{1}{z}\left(-0.405182\Phi_p - 0.459468\Phi_p^2 + 0.0507105\Phi_p^3\right), \end{aligned} \tag{4.22}$$

which is consistent with (4.14) if we approximate $2\Delta \approx 1$. In Ref.[14] we determined an interpolation formula for the leading term with the correct large-Φ_p behavior. Here we do the same for the correction term: we determine an interpolation formula that has the asymptotic behavior (4.15) for $\Phi_p \to \infty$ with α given by Eq. (4.16), and agrees with the previous expansion for $\Phi_p \to 0$. A simple expression satisfying these two properties is

$$-0.405182\Phi_p(1 + 2.30016\Phi_p + 1.08734\Phi_p^2)^{0.493}\ . \tag{4.23}$$

Combining this expression with that obtained in Ref.[14] we obtain for the compressibility factor

$$Z = \left(\frac{1 + 1.52605\Phi_p + 0.795366\Phi_p^2}{1 + 0.5245\Phi_p}\right)^{1.311} - \frac{0.405182}{z^{2\Delta}}\Phi_p(1 + 2.30016\Phi_p + 1.08734\Phi_p^2)^{0.493}. \tag{4.24}$$

It is not possible to determine *a priori*, for each z, the density range $\Phi_p \lesssim \Phi_{p,\max}(z)$ in which Eq. (4.24) applies. For $\Phi_p = 1$ we can compare expression (4.24) with the virial expansion (3.2) including the terms up to $n = 4$. The relative difference is less than 5% (1%, 0.1% respectively) for $z \gtrsim 1.7$ (4, 12 respectively). Thus, for $\Phi_p = 1$, Eq. (4.24) is substantially correct for $z \gtrsim 4$ and reasonably predictive for $z \gtrsim 2$. Accepting an error of 5% (it makes little sense to require a smaller error since our interpolation formulas cannot in any case be more precise than 5-10%; see the discussion reported in Ref.[14]), we can set $\Phi_{p,\max}(z = 2) = 1$. An estimate of $\Phi_{p,\max}(z)$ for larger values of z can be obtained by noting that

$$\Phi_{p,\max}(z) \sim z^{6\nu-2} \sim z^{2.53}. \tag{4.25}$$

Indeed, Eq. (4.24) is valid as long as $z \gg c\ell^3 N^{3/2} \sim c\hat{R}_g^3\alpha_g^{-3} \sim \Phi_p\alpha_g^{-3}$. Hence, since $\alpha_g \sim z^{2\nu-1}$ for large z, we obtain Eq. (4.25). Therefore, with errors at most of 5% we expect the range to extend up to $\Phi_{p,\max}(z) \approx (z/2)^{2.53}$.

The prediction (4.24) for $\Phi_p \leq 10$ is reported in Fig. 7 for several values of z. It is clear that the results for $z = 2$ do not extend beyond $\Phi_p = 1$, since, by increasing Φ_p, Z begins to bend in an unphysical way. No such phenomenon is observed for $z \gtrsim 5$, which is therefore expected to be the range of z in which (4.24) applies for $\Phi_p \lesssim 10$. This is in agreement with the estimate of $\Phi_{p,\max}(z)$ given above. Note that scaling corrections are quite large in the semidilute regime. For instance, consider $z = 10$. Since $A_2/A_2^* = \Psi/\Psi^* = 0.97$, in the dilute regime the solution is essentially in good-solvent conditions. For $\Phi_p = 10$ we obtain $Z = 31.3$ to be compared with the good-solvent value $Z_{GS} = 35.8$: the pressure is lower by 14%, a significant deviation from the good-solvent value.

D. Concentration dependence of the polymer size

The considerations we have presented for the osmotic pressure can be generalized to the radii. Deep in the semidilute region, polymers behave like ideal chains and therefore R^2 behaves as

$$R^2 = N\ell^2 f_R(w/c_m) = N\ell^2 f_R\left(\frac{z}{c\ell^3 N^{3/2}}\right), \tag{4.26}$$

with $f_R(0) \neq 0$. As before, we focus on the deviations from the good-solvent regime. If R is the end-to-end distance or the radius of gyration, corrections scale as $z^{-2\Delta}$ (this is not the case for the hydrodynamic radius which may show additional corrections proportional to[15,31] $z^{4\nu-4}$). In order to obtain the behavior for large c in the good-solvent regime we write

$$R^2 = a_R\hat{R}^2\Phi_p^{\alpha_1}(1 + b_R z^{-2\Delta}\Phi_p^{\alpha_2}), \tag{4.27}$$

and require this expression to be consistent with Eq. (4.26). This allows us to identify α_1 and α_2:

$$\alpha_1 = -\frac{2\nu - 1}{3\nu - 1} \qquad \alpha_2 = \frac{\Delta}{3\nu - 1}. \tag{4.28}$$

Using these expressions, we can now extrapolate our virial results to the whole semidilute region, obtaining (the leading terms already appear in Ref.[15])

$$\frac{R_e^2}{\hat{R}_e^2} = (1 + 0.801\Phi_p + 0.37\Phi_p^2)^{-0.115} - \frac{1}{z^{2\Delta}}0.024\Phi_p(1 + 0.76\Phi_p)^{-0.554}, \tag{4.29}$$

$$\frac{R_g^2}{\hat{R}_g^2} = (1 + 0.655\Phi_p + 0.28\Phi_p^2)^{-0.115} - \frac{1}{z^{2\Delta}}0.021\Phi_p(1 + 1.46\Phi_p)^{-0.554}. \tag{4.30}$$

As discussed before, these expressions are only valid for $z \ll c\ell^3 N^{3/2}$. We do not present an extrapolation for R_H, because of the presence of two different corrections (one proportional to $z^{-2\Delta}$ and one proportional to $z^{4\nu-4}$, see Ref.[31]), which make extrapolations of the form (4.27) incorrect. The results for $R_g^2/\hat{R}_g^2$ are shown in Fig. 8 for the same values of z that occur in Fig. 7. Note that for large z, our extrapolation predicts $R_g^2/\hat{R}_g^2$ to decrease when z decreases. This is consistent with the nonmonotonic behavior of $S_{1,g}(z)$ we mentioned in Sec. IV B and with the numerical results of Ref.[15], which suggest a negative scaling correction for $S_{2,g}(z)$: $S_{2,g}(z) = -0.087 - (0.003 \pm 0.005)z^{-2\Delta}$. Of course, this behavior should eventually change, since $R_g^2/\hat{R}_g^2$ should converge to 1 as $z \to 0$.

For the radius of gyration corrections are less evident than in the case of Z. For instance, for $\Phi_p = 10$ the relative difference between $R_g^2/\hat{R}_g^2$ for $z = 10$ and for $z = \infty$ (good-solvent value) is only of 0.7%, indicating that the polymer size is less sensitive to the solvent quality far from the ideal-chain limit.

E. Comparison with previous renormalization-group results

In the previous sections we have obtained predictions for the osmotic pressure and the radii in the TPM. We wish now to compare these results with those obtained by using field theory. We compare mainly with the results reported in Ref.[5], which have been obtained by using renormalized one-loop perturbative expressions with a careful choice of the renormalization constants. In Fig. 9 we report the compressibility factor Z as a function of z for $\Phi_p = 1$, i.e. for the largest value of the density at which the virial expansion is supposed to work. As we discussed in Ref.[14] this expression should be quite accurate, deviations being at most of 1-2%. We also report the field-theoretical result, which is in perfect agreement with our estimate. For larger values of Φ_p we cannot use the virial expansion. Instead, we employ the approximate expression (4.24), which is valid only for large values of z. In Fig. 10 we report Z in the range $0 \le \Phi_p \le 10$ for two values of z: $z = 9.90$ corresponding to $R \equiv 1 - \Psi/\Psi^* = 0.03$ and $z = 5.79$ corresponding to $R = 0.05$. We report our expression (4.24) and the field-theoretical prediction of Ref.[5]. For $R = 0.03$, our result is in very good agreement with the field-theoretical one. On the other hand, for $R = 0.05$, we observe significant differences for $\Phi_p \gtrsim 5$. In any case, these discrepancies are within the 5% error we expect on our extrapolations. Indeed, for $\Phi_p = 5$ we predict $Z_{GS} = 15.0$ and $Z(z = 5) = 12.9$ to be compared with the field-theory results $Z_{GS} = 14.5$ and $Z(z = 5) = 12.7$; for $\Phi_p = 10$ we obtain $Z_{GS} = 35.9$ and $Z(z = 5) = 28.5$ to be compared with $Z_{GS} = 34.2$ and $Z(z = 5) = 28.4$. In all cases differences are less than 5%. Finally, note that both field theory and our results predict Z to be significantly lower than the good-solvent value Z_{GS} for $\Phi_p \gtrsim 1$ as soon as R is different from zero.

A phenomenological expression for Z as a function of c and $R = 1 - \Psi/\Psi^*$ is also reported in Refs.[35,36]. For $\Phi_p \lesssim 1$ there is good agreement[37] with our results for all values of R, differences being less than 1%. On the other hand, significant differences are observed for larger values of Φ_p.[37] For instance, for $R = 0.03$ and $\Phi_p = 10$ we predict $Z/Z_{GS} - 1 = -0.118$, Ref.[5] gives -0.113, in substantial agreement with our result, while the expression reported in Ref.[35] gives -0.060, which differs by a factor of 2.

It is also interesting to compare the results for $R_g^2/\hat{R}_g^2$. In Fig. 11 we report this ratio for $\Phi_p = 1$ as a function of z, together with the one-loop prediction of Ref.[5]. In the good-solvent regime the difference is quite large. The poor behavior of the field-theoretical expressions in the dilute regime can be explained by looking at the virial expansion of R_g^2 for $z \to \infty$. In the good-solvent regime, the Monte Carlo simulations of Ref.[15] give $S_{1,g}^* \approx -0.315$, $S_{2,g}^* \approx -0.09$, while Ref.[5] predicts $S_{1,g}^* \approx -1.19$, $S_{2,g}^* \approx 5.74$. One-loop perturbation theory renormalized as in Ref.[5] seems to be unable to reproduce correctly the polymer size as a function of Φ_p, at variance with what occurs for Z. This is not totally surprising since the nonuniversal parameters that enter in the perturbative predictions (c_0 and n_0 in the notation of Ref.[5]) were tuned to reproduce accurately the thermodynamic behavior.[38] For instance, a different resummation of one-loop perturbation theory (see Sec. 6 of Ref.[39]) gives $S_{1,g}^* \approx -0.145$, $S_{2,g}^* \approx 0.0738$, which are much closer to the Monte Carlo results.

V. CONCLUSIONS

In this paper we have determined the explicit TPM expressions for several quantities which characterize polymer solutions in the dilute regime. First, we have determined the universal constants $A_n(z)$ for $n = 2, 3, 4$. This allows us to obtain precise predictions for the osmotic pressure in terms of the polymer packing fraction Φ_p in the dilute regime $\Phi_p \lesssim 1$. Then, we have computed the swelling factors for three different radii that characterize the polymer size. Finally, we have studied their concentration dependence.

The expressions we have determined in this paper can be used in two different contexts. First, they provide expressions that may be used to fit the experimental data outside the universal (large-N) regime. Note that the range of values of N in which a given system approximately behaves as predicted by the TPM expressions is nonuniversal, and thus in some cases the agreement is only at the level of the leading behavior, while in some others it may cover a significant range of polymer lengths. For instance, in some systems (e.g., in PMMA in chloroform or nitroethane at 20 °C) the interpenetration ratio approaches the universal value from above, i.e. $\Psi > \Psi^*$ for large N (in the terminology of Ref.[5], these systems are "strong-coupling systems"). This type of behavior cannot be described by the TPM expressions we have derived here which predict that the approach is always from below. In some other systems ("weak-coupling systems") instead, the TPM expressions describe quite well the experimental behavior (for instance, polystyrene in cyclohexane or transdecaline, see chapter 15 in Ref.[5]). Note also that Ψ is generically a decreasing function of the temperature (at $T \to T_\theta$, $\Psi \to 0$) and thus a strong-coupling system becomes a weak-coupling system as T is lowered and thus eventually one can use the TPM to interpret the experimental behavior.

The use of the TPM to describe the nonasymptotic behavior for finite values of N is mainly phenomenological and rigorously justified only in systems in which the persistence length is larger than the typical monomer size.[13] A second use of the TPM expressions is in the description of the crossover to the θ point. As we have explained in the introduction, the crossover functions defined in Eq. (1.1) can be computed in the TPM, by identifying z with $(T - T_\theta)N^{1/2}(\ln N)^{-4/11}$ (modulo a normalization multiplicative constant). However, this identification is valid only close to the θ point, since it assumes $T - T_\theta \ll 1$. To avoid this limitation, one can proceed as suggested in Refs.[9,29], i.e., one can parametrize the crossover in terms of a physical variable. For instance, one can use the interpenetration ratio Ψ. Eq. (1.1) can then be written as

$$\mathcal{O}(T, N, c) = \alpha_1 \mathcal{O}_G(N, c) f_{\mathcal{O}}(\Psi, c\hat{R}_g^3). \tag{5.1}$$

The *quality* of the solution is now characterized by Ψ that varies between 0 (poor solvent) and Ψ^* (good solvent). In Fig. 12 we report the quantities computed above as a function of Ψ/Ψ^*. Note that both A_n and $S_{n,\#}$ are small up to $\Psi/\Psi^* \approx 0.3$ and also the swelling factors α do not change significantly in this range. This means that, for $\Psi \lesssim 0.3\Psi^* \approx 0.08$, polymers behave approximately as Gaussian coils. Of course, as $T \to T_\theta$ three-body forces become increasingly important and thus tricritical corrections should be included. In the opposite range $\Psi \gtrsim 0.08$ tricritical effects can be neglected (see the numerical data in Ref.[9]) and one can use the TPM expressions to describe the polymer behavior.

The authors thank Tom Kennedy for providing his efficient simulation code for lattice self-avoiding walks.

APPENDIX A: PERTURBATIVE CALCULATIONS

In this appendix we report the one-loop TPM expressions for the quantities reported in this paper. We use the general results of Ref.[39]. For the osmotic pressure we start from the one-loop expression

$$\frac{\beta\Pi}{c} = 1 + \frac{u}{2}cn^2 - \frac{1}{2c}\int \frac{d^3p}{(2\pi)^3} \ln[1 + 2cu\Gamma^{(2)}(p)] + u \int \frac{d^3p}{(2\pi)^3} \frac{\Gamma^{(2)}(p)}{1 + 2cu\Gamma^{(2)}(p)}, \tag{A1}$$

where u is the coupling constant and n is the polymer length. They are related to z and R_g by

$$z = (2\pi)^{-3/2} u n^{1/2} \qquad \hat{R}_g^2 = \frac{n}{2} + O(u). \tag{A2}$$

The function $\Gamma^{(2)}(p)$ is the Debye function:

$$\frac{1}{n^2}\Gamma^{(2)}(p) = \frac{2}{p^2 n} - \frac{4}{(p^2 n)^2}(1 - e^{-p^2 n/2}). \tag{A3}$$

Expanding in powers of c we obtain A_4:

$$A_4(z) = \frac{131072}{45045}(14075 + 12624\sqrt{2} - 18468\sqrt{3})\pi^{9/2} z^4 + O(z^5) = -29883.1 z^4 + O(z^5). \tag{A4}$$

We give also numerical values for the leading TPM contributions to the following virial coefficients:

$$
\begin{aligned}
A_5(z) &= 932283 z^5, && \text{(A5)}\\
A_6(z) &= -3.13006\cdot 10^7\, z^6, && \text{(A6)}\\
A_7(z) &= 1.10136\cdot 10^9\, z^7, && \text{(A7)}\\
A_8(z) &= -4.00539\cdot 10^{10}\, z^8, && \text{(A8)}\\
A_9(z) &= 1.49307\cdot 10^{12}\, z^9, && \text{(A9)}\\
A_{10}(z) &= -5.67361\cdot 10^{13}\, z^{10}. && \text{(A10)}
\end{aligned}
$$

We can also compute the radius of convergence of the virial expansion. A simple analysis of the integral (A1) shows that the singularity in the complex c-plane that is closest to the origin corresponds to $cun^2 = -1$. This implies $A_n/A_{n-1} = -8\pi^{3/2}z$ asymptotically, and that the virial expansion converges for $|\Phi_p| < 1/(8\pi^{3/2}z)$ in the limit $z \to 0$.

Using the expressions reported in Ref.[39] we obtain for the radius of gyration:

$$
\begin{aligned}
S_{1,g}(z) &= \frac{64}{3465}(1365 - 1028\sqrt{2})\pi^{3/2}z^2 = -9.13421 z^2, && \text{(A11)}\\
S_{2,g}(z) &= \frac{2048}{405405}(85013 - 115408\sqrt{2} + 45684\sqrt{3})\pi^3 z^3 = 145.428 z^3, && \text{(A12)}\\
S_{3,g}(z) &= -3113.85 z^4, && \text{(A13)}\\
S_{4,g}(z) &= 78503.4 z^5, && \text{(A14)}\\
S_{5,g}(z) &= -2.19663\cdot 10^6\, z^6. && \text{(A15)}
\end{aligned}
$$

For the end-to-end distance we obtain analogously:

$$
\begin{aligned}
S_{1,e}(z) &= \frac{128}{315}(103 - 76\sqrt{2})\pi^{3/2}z^2 = -10.1374 z^2, && \text{(A16)}\\
S_{2,e}(z) &= \frac{4096}{10395}(1427 - 3248\sqrt{2} + 1836\sqrt{3})\pi^3 z^3 = 167.132 z^3, && \text{(A17)}\\
S_{3,e}(z) &= -3654.20 z^4, && \text{(A18)}\\
S_{4,e}(z) &= 93359.1 z^5, && \text{(A19)}\\
S_{5,e}(z) &= -2.6358\cdot 10^6\, z^6. && \text{(A20)}
\end{aligned}
$$

Finally, for the hydrodynamic radius we use the representation

$$
\frac{1}{R_H} = 4\pi \int \frac{d^3q}{(2\pi)^3}\frac{F(q)}{q^2}, \qquad \text{(A21)}
$$

where $F(q)$ is the form factor

$$
F(q) = \frac{1}{N^2}\left\langle \sum_{ij} e^{i\mathbf{q}\cdot(\mathbf{r}_i - \mathbf{r}_j)} \right\rangle, \qquad \text{(A22)}
$$

which is normalized so that $F(q) = 1 - \frac{q^2}{3}R_g^2 + O(q^4)$. For the density corrections, we obtain at leading order

$$
\begin{aligned}
S_{1,H}(z) &= 3.32047 z^2 + O(z^3)\ , && \text{(A23)}\\
S_{2,H}(z) &= -44.8425 z^3 + O(z^4)\ . && \text{(A24)}
\end{aligned}
$$

Finally, we report the swelling factors:

$$
\begin{aligned}
\alpha_e^2 &= 1 + \frac{4}{3}z + O(z^2), && \text{(A25)}\\
\alpha_g^2 &= 1 + \frac{134}{105}z + O(z^2), && \text{(A26)}\\
\alpha_H &= 1 - \left(\frac{27\pi}{16} - 4 - \frac{3\pi}{2}\log\frac{3}{2}\right) z + O(z^2)\ . && \text{(A27)}
\end{aligned}
$$

Additional terms for α_e^2 are reported in Ref.[13].

---

[1] P. G. de Gennes, Phys. Lett. **38A**, 339 (1972).

[2] P. G. de Gennes, *Scaling Concepts in Polymer Physics* (Cornell University Press, Ithaca, NY, 1979).

[3] K. F. Freed, *Renormalization Group Theory of Macromolecules* (Wiley, New York, 1987).

[4] J. des Cloizeaux and G. Jannink, *Polymers in Solution: Their Modelling and Structure* (Clarendon, Oxford, 1990).

[5] L. Schäfer, *Excluded Volume Effects in Polymer Solutions* (Springer Verlag, Berlin, 1999).

[6] At present the most accurate estimates of ν are $\nu = 0.58758 \pm 0.00007$ (Ref.[24]), $\nu = 0.5874 \pm 0.0002$ [T. Prellberg, J. Phys. A **34**, L599 (2001)], $\nu = 0.58765 \pm 0.00020$ [H.-P. Hsu, W. Nadler, and P. Grassberger, Macromolecules **37**, 4658 (2004)], $\nu = 0.5876 \pm 0.0002$ (Ref.[26]), $\nu = 0.5876 \pm 0.0002$ [N. Clisby, R. Liang, and G. Slade, J. Phys. A **40**, 10973 (2007)] (assuming $0.50 \le \theta \le 0.53$). For an extensive list of results, see A. Pelissetto and E. Vicari, Phys. Rept. **368**, 549 (2002).

[7] The θ transition is usually a liquid transition between the coil state and the globular state and it may be of first or of second order. For particularly stiff polymers, the globular state is absent and one observes a direct transition to a solid crystalline phase. See, e.g., F. Rampf, W. Paul, and K. Binder, Europhys. Lett. **70**, 628 (2005), J. P. K. Doye, R. P. Sear, and D. Frenkel, J. Chem. Phys. **108**, 2134 (1998), and references therein.

[8] B. Duplantier, J. Phys. (France) **43**, 991 (1982); **47**, 745 (1986); J. Chem. Phys. **86**, 4233 (1987).

[9] A. Pelissetto and J.-P. Hansen, J. Chem. Phys. **122**, 134904 (2005).

[10] A. D. Sokal, Europhys. Lett. **27**, 661 (1994); erratum **30**, 123 (1995).

[11] H. Yamakawa, *Modern Theory of Polymer Solutions* (Harper–Row, New York, 1971).

[12] B. H. Zimm, W. H. Stockmayer, and M. Fixman, J. Chem. Phys. **21**, 1716 (1953).

[13] S. Caracciolo, M. S. Causo, A. Pelissetto, P. Rossi, and E. Vicari, Phys. Rev. E **64**, 046130 (2001).

[14] S. Caracciolo, B. M. Mognetti, and A. Pelissetto, J. Chem. Phys. **125**, 094903 (2006).

[15] S. Caracciolo, B. M. Mognetti, and A. Pelissetto, J. Chem. Phys. **125**, 094904 (2006); (erratum) **126**, 169901 (2007).

[16] C. Domb and G. S. Joyce, J. Phys. C **5**, 956 (1972).

[17] M. Lal, Molec. Phys. **17**, 57 (1969).

[18] B. MacDonald, N. Jan, D. L. Hunter, and M. O. Steinitz, J. Phys. A **18**, 2627 (1985).

[19] N. Madras and A. D. Sokal, J. Stat. Phys. **50**, 109 (1988).

[20] A. D. Sokal, in *Monte Carlo and Molecular Dynamics Simulations in Polymer Science*, edited by K. Binder (Oxford Univ. Press, Oxford, 1995).

[21] T. Kennedy, J. Stat. Phys. **106**, 407 (2002).

[22] S. Caracciolo, G. Parisi, and A. Pelissetto, J. Stat. Phys. **77**, 519 (1994).

[23] A. J. Barrett and C. Domb, Proc. Roy. Soc. London A **367**, 143 (1979).

[24] P. Belohorec and B.G. Nickel, "Accurate universal and two-parameter model results from a Monte-Carlo renormalization group study," Guelph University report (1997), unpublished.

[25] In experimental work the low-density behavior of the osmotic pressure Π is usually written as $\Pi/(RT\rho) = 1/M + B_2\rho + O(\rho^2)$, where M is the molar mass of the polymer, ρ the weight concentration, and T the absolute temperature. Then, $\Psi \equiv 2(4\pi)^{-3/2} M^2 B_2 \hat{R}_g^{-3}/N_A$, where N_A is the Avogadro number.

[26] A. Pelissetto and E. Vicari, J. Phys. A **40**, F539 (2007).

[27] To prove that $a_n/a_2 = b_n$, we write $A_n = A_n^* + A_{1,n}(w)N^{-\Delta}$. For $w \to 0$, consistency with Eq. (3.9) requires $A_{1,n}(w) = a_n(kw)^{-2\Delta}$, where k is defined by $z = kwN^{1/2}$. Since $A_{1,n}(w)/A_{1,2}(w) = b_n$ for any n, we obtain $a_n/a_2 = b_n$.

[28] M. Muthukumar and B. G. Nickel, J. Chem. Phys. **86**, 460 (1987).

[29] B. G. Nickel, Macromolecules **24**, 1358 (1991).

[30] E. F. Casassa, Pure Appl. Chemistry **31**, 151 (1972).

[31] B. Dünweg, D. Reith, M. Steinhauser, and K. Kremer, J. Chem. Phys. **117**, 914 (2002).

[32] In general, one expects corrections of order $N^{-n/2}$, n integer, with additional logarithmic factors (Ref.[24]).

[33] We relate the constant $\tilde{z}$ of Ref.[5] to z by requiring $A_2(z) \approx \frac{1}{2}(4\pi)^{3/2} z$ for $z \to 0$: we obtain $z = 0.182\tilde{z}$.

[34] J. F. Douglas and K. F. Freed, Macromolecules **17**, 1854 (1984).

[35] L. Lue and S. B. Kiselev, Intern. J. Thermophys. **23**, 117 (2002).

[36] L. Lue, J. Chem. Phys. **112**, 3442 (2000).

[37] The compressibility factor Z in Refs.[35,36] is expressed in terms of $X \equiv B_2 c$, where B_2 is the second virial coefficient defined by $Z = 1 + B_2 c + O(c^2)$. In order to relate X to Φ_p we note that $X = A_2 c \hat{R}_g^3 = A_2^*(\Psi/\Psi^*) 3\Phi_p/(4\pi)$ and use $A_2^* = 5.500$ (Ref.[14]).

[38] It is possible to riduce the discrepancy between field theory and our results by changing the parameters c_0 and n_0. For the values suggested in Ref.[5], $c_0 = 1.2$ and $n_0 = 0.53$, $R_g^2/\hat{R}_g^2 = 0.857$ for $\Phi_p = 1$, to be compared with our result 0.920. The discrepancy decreases if c_0 is increased: for $n_0 = 0.53$ and $c_0 = 6.9$ field theory gives the

same result as ours. However, c_0 cannot be too large, otherwise Z is underestimated in the semidilute regime. For $c_0 = 6.9$, field theory predicts $Z = 1.20\Phi_p^{1.309}$, while experiments, other field-theory calculations, and the extrapolation of the virial expansion predict $Z = a\Phi_p^{1.31}$ with $a = 1.5$-1.7 (see the conclusions of Ref.[14] for a summary of the existing results).

[39] T. Ohta and A. Nakanishi, J. Phys. A **16**, 4155 (1983).

TABLE I: Estimates of $A_2(z)$ for five different values of z and different $N_{\min}$.

z	$N_{\min} = 100$	$N_{\min} = 250$	$N_{\min} = 500$	$N_{\min} = 1000$
$z_1 = 0.056215$	0.99241(41)	0.99212(59)	0.99257(98)	0.9906(19)
$z_2 = 0.148726$	1.97964(79)	1.9796(12)	1.9782(18)	1.9831(35)
$z_3 = 0.321650$	2.9646(11)	2.9649(16)	2.9621(27)	2.9642(48)
$z_4 = 0.728877$	3.9469(14)	3.9452(21)	3.9433(34)	3.9498(65)
$z_5 = 2.508280$	4.9264(15)	4.9221(23)	4.9147(36)	4.9169(65)

TABLE II: TPM estimates of several quantities for five different values of z. z_1, z_2, z_3, z_4, and z_5 are reported in the text.

	z_1	z_2	z_3	z_4	z_5
A_2	0.99257(98)	1.9782(18)	2.9621(27)	3.9433(34)	4.9147(36)
A_3	0.08486(78)	0.6061(30)	1.8435(82)	4.021(13)	7.243(22)
A_4	−0.095(11)	−0.857(78)	−2.77(30)	−5.51(79)	−10.3(1.8)
A_{ge}	0.166145(65)	0.165517(62)	0.164591(65)	0.163272(62)	0.161514(55)
A_{gH}	1.50553(84)	1.50964(90)	1.51731(78)	1.52597(74)	1.54165(69)
$S_{1,g}$	−0.01711(66)	−0.0630(11)	−0.1278(18)	−0.1970(24)	−0.2747(25)
$S_{2,g}$	0.0073(12)	0.0309(42)	0.051(10)	0.082(17)	−0.002(25)
$S_{1,e}$	−0.01931(71)	−0.0718(13)	−0.1469(20)	−0.2340(27)	−0.3301(30)
$S_{2,e}$	0.0097(14)	0.0381(53)	0.083(12)	0.124(21)	0.035(33)
$S_{1,H}$	0.00527(36)	0.02079(75)	0.0405(11)	0.0602(13)	0.0771(15)
$S_{2,H}$	−0.00197(84)	−0.0086(33)	−0.0041(66)	0.026(12)	0.028(17)
α_e^2	1.06872(81)	1.16553(82)	1.31167(92)	1.5683(12)	2.2283(15)
α_g^2	1.06545(71)	1.15751(78)	1.29540(89)	1.5362(11)	2.1595(13)
α_H	1.03127(44)	1.07196(44)	1.12878(42)	1.22196(40)	1.43419(43)

TABLE III: TPM interpolation formulas.

$A_2(z)$	$4\pi^{3/2}z(1 + 19.1187z + 126.783z^2 + 331.99z^3 + 268.96z^4)^{-1/4}$
$A_3(z)$	$1100.7z^3(1 + 23.1258z + 195.358z^2 + 594.386z^3 + 541.906z^4)^{-3/4}$
$A_4(z)$	$-29883.1z^4(1 + 17.4354z + 135.853z^2 + 437.409z^3)^{-4/3}$
$A_{ge}(z)$	$1/6 - 0.0571429z(1 + 1455.41z + 47738.2z^2 + 584.595z^3 + 5025.99z^4)^{-1/4}$
$A_{gH}(z)$	$1.50451 + 0.0288252z(1 - 1.64436z + 1.57777z^2 + 0.0535093z^3)^{-1/3}$
$S_{1,g}(z)$	$-9.13421(1 + 0.0182093z)z^2/(1 + 10.8944z + 28.8313z^2 + 0.52769z^3)$
$S_{2,g}(z)$	$145.428(1 - 0.39868z)z^3(1 + 25.0806z + 92.4415z^2 + 131.164z^3)^{-4/3}$
$S_{1,e}(z)$	$-10.1374(1 + 0.0164091z)z^2/(1 + 10.8171z + 26.1977z^2 + 0.431731z^3)$
$S_{2,e}(z)$	$167.132(1 - 0.161819z)z^3(1 + 24.6508z + 52.9313z^2 + 178.051z^3)^{-4/3}$
$S_{1,H}(z)$	$3.32047z^2(1 + 23.196z + 71.9449z^2 + 257.679z^3)^{-2/3}$
$S_{2,H}(z)$	$-44.8425(1 - 2.7513z)z^3(1 + 28.5327z - 37.0818z^2 + 350.101z^3)^{-4/3}$
$\alpha_g(z)$	$(1 + 10.9288z + 35.1869z^2 + 30.4463z^3)^{0.0583867}$
$\alpha_e(z)$	$(1 + 11.4181z + 39.7661z^2 + 42.8257z^3)^{0.0583867}$
$\alpha_H(z)$	$(1 + 10.4351z + 29.7693z^2 + 16.8909z^3)^{0.0583867}$

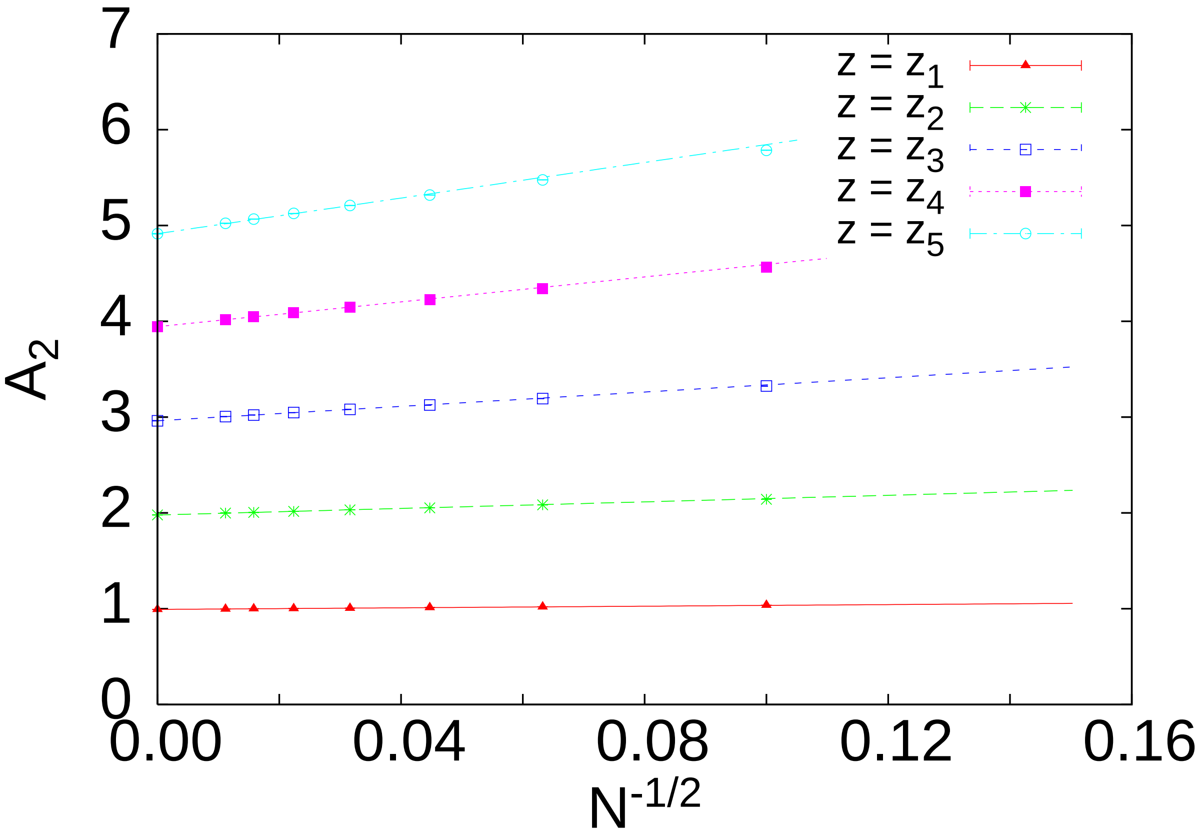

FIG. 1: The invariant ratio A_2 as a function of $N^{-1/2}$ for the five values of z reported in the text. We also report the linear extrapolation as determined by the fit of all data.

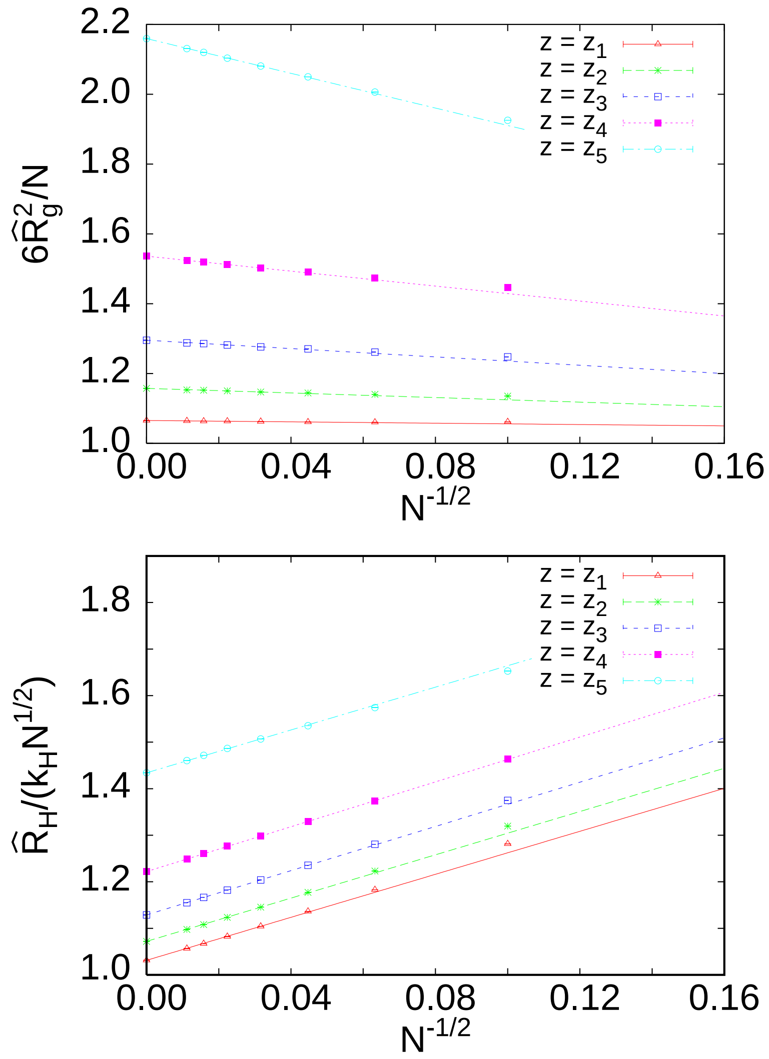

FIG. 2: The ratios $6\widehat{R}_g^2/N$ and $\widehat{R}_H/(k_H\sqrt{N})$ (they converge to α_g^2 and α_H, respectively) as a function of $N^{-1/2}$ for the five values of z reported in the text. We also report the linear extrapolation as determined by the fit of all data.

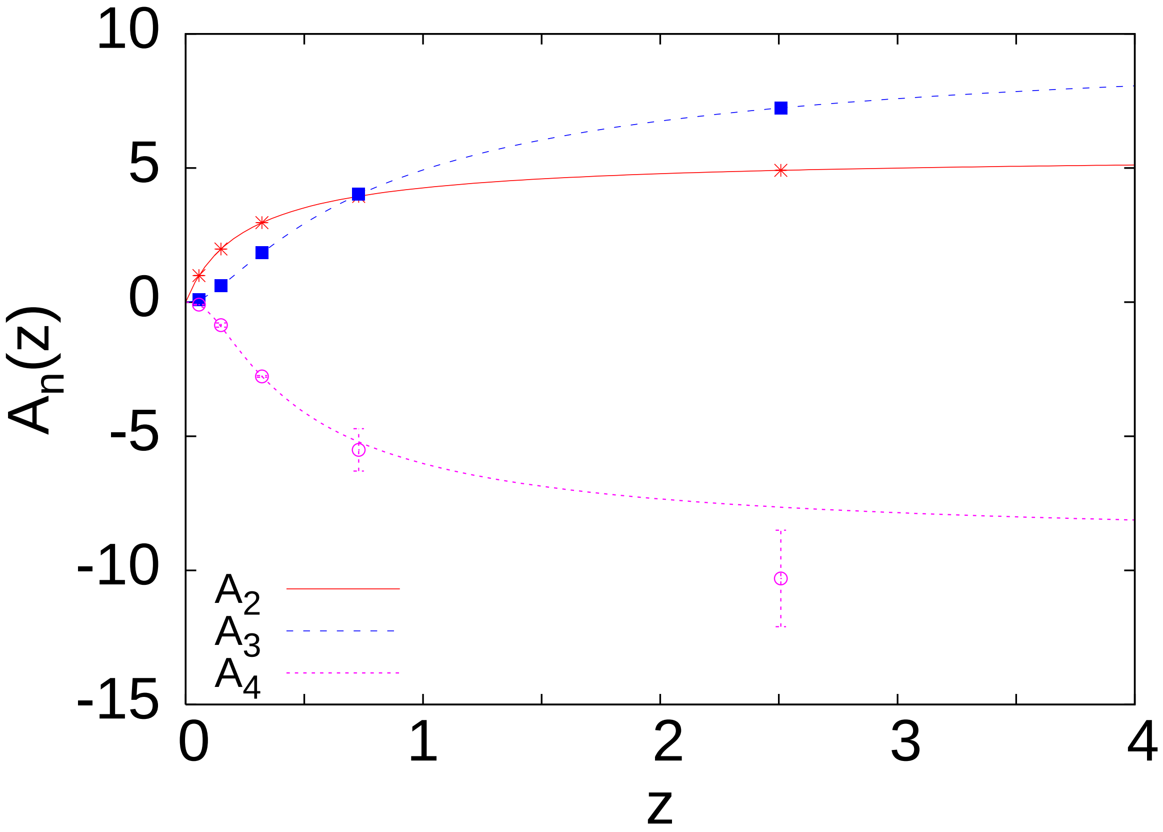

FIG. 3: The TPM functions for the virial coefficients. We also show the Monte Carlo results reported in Table II.

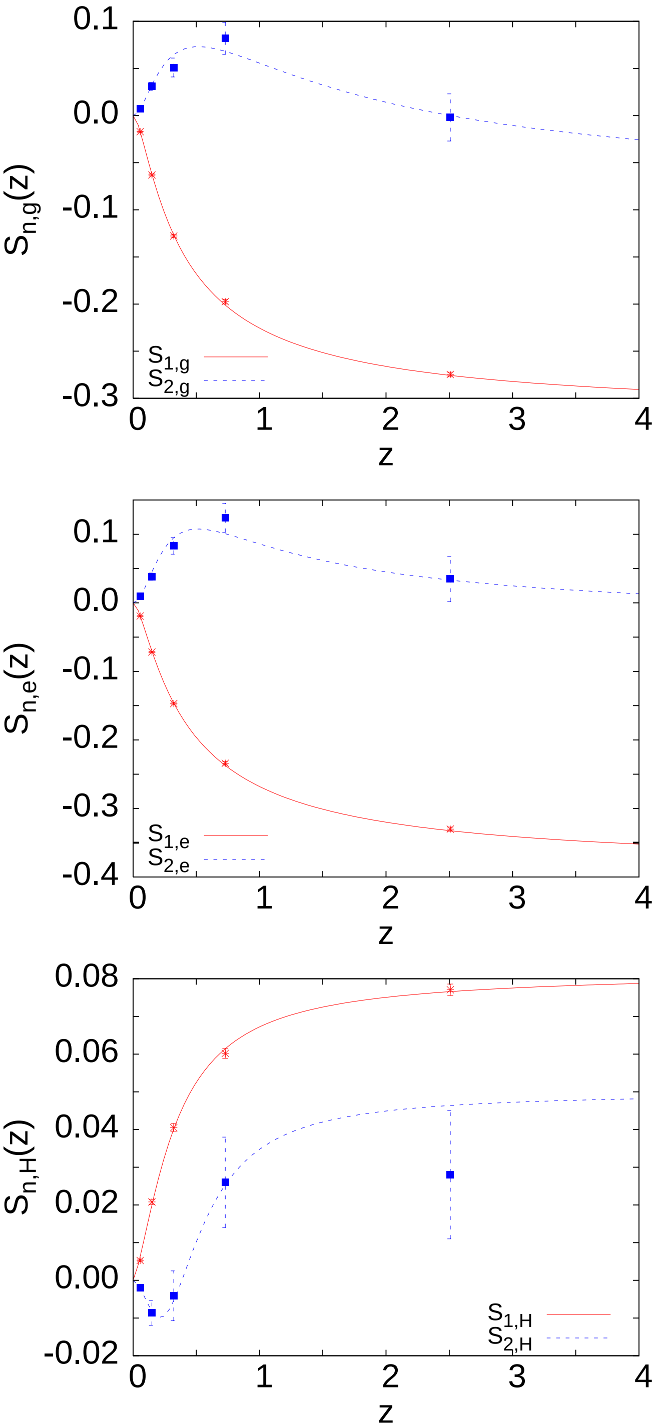

FIG. 4: The TPM functions for the density coefficients $S_{n,g}$, $S_{n,e}$, and $S_{n,H}$. We also report the Monte Carlo results reported in Table II.

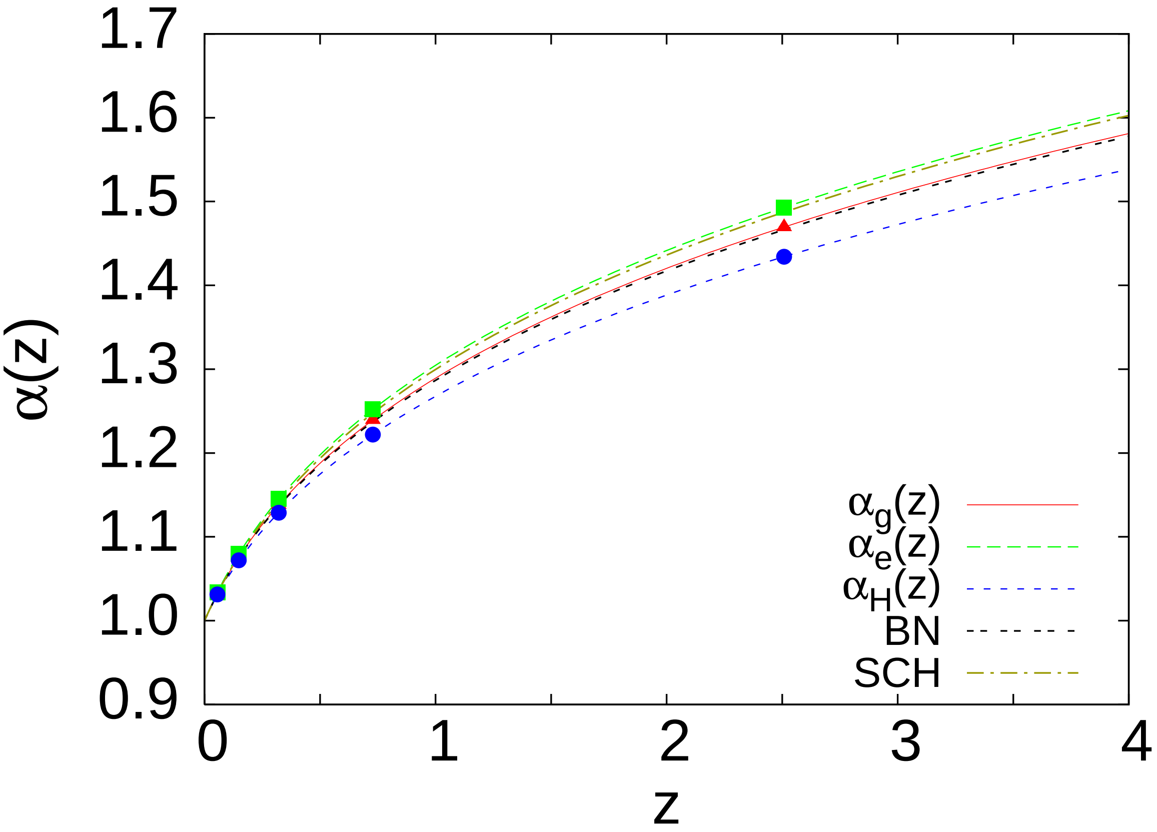

FIG. 5: The TPM functions for the swelling factors. Together with our predictions we also report the results of Ref.[5] (SCH) and of Ref.[24] (BN) for $\alpha_g(z)$. Squares, triangles, and circles correspond respectively to the Monte Carlo results for α_e, α_g, and α_H (see Table II).

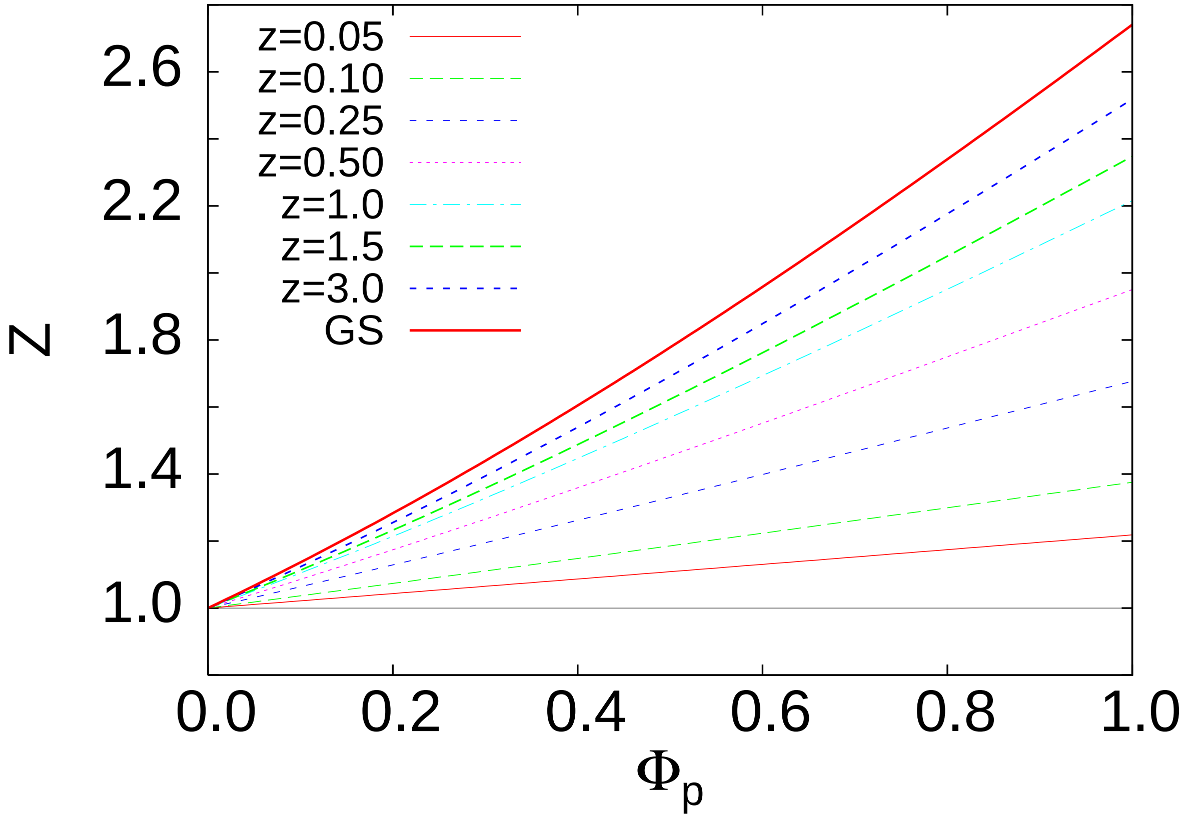

FIG. 6: The compressibility factor vs Φ_p for several values of z in the dilute region.

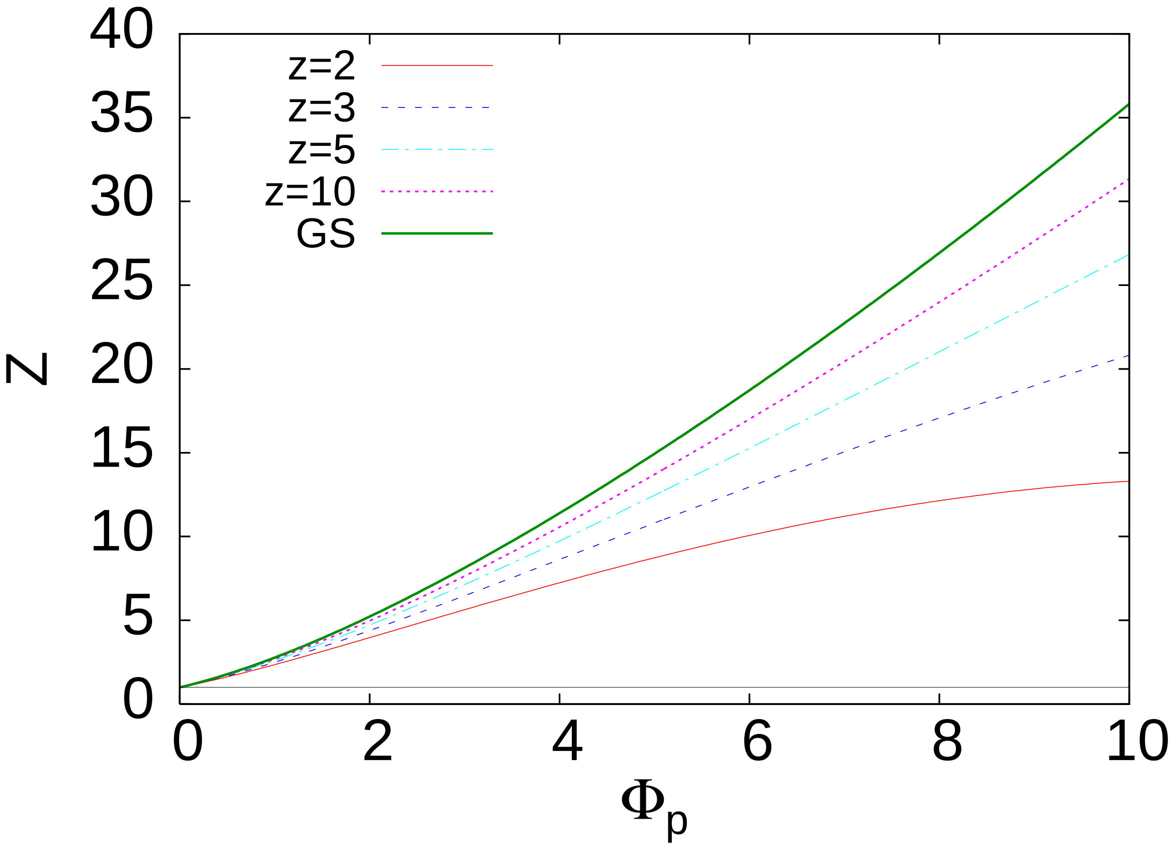

FIG. 7: The compressibility factor vs Φ_p for several values of z in the semidilute region.

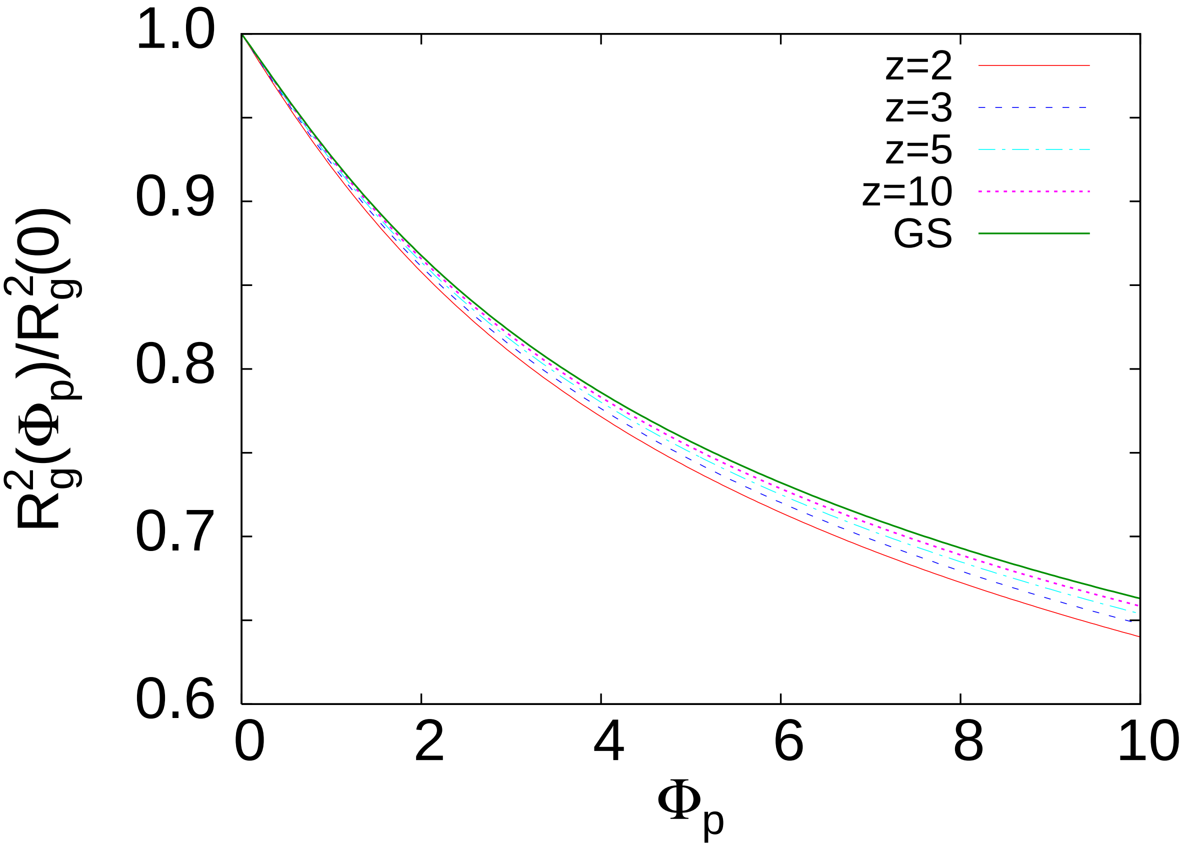

FIG. 8: Ratio $R_g^2/\hat{R}_g^2$ for the radius of gyration for several values of z in the semidilute region.

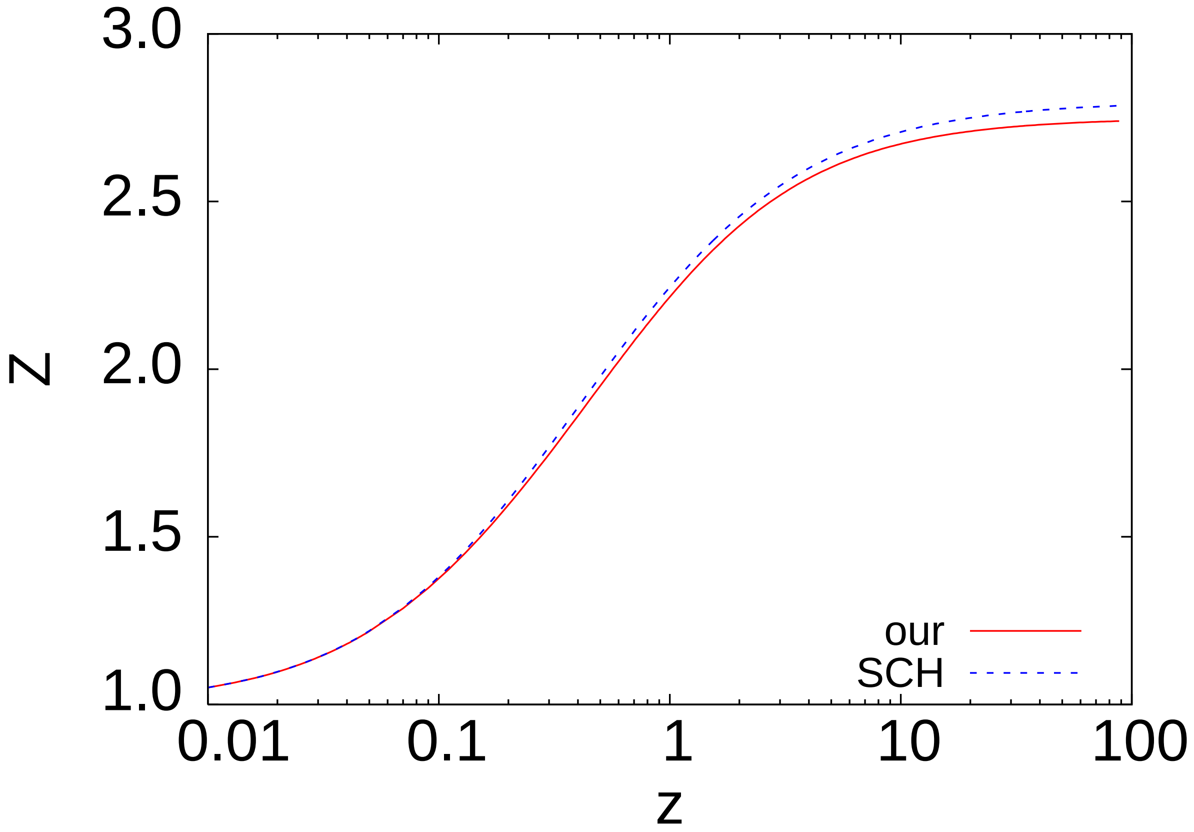

FIG. 9: The compressibility factor Z at $\Phi_p = 1$ as a function of z. We report our results (”our”) and the field-theoretical ones reported in Ref.[5] (”SCH”).

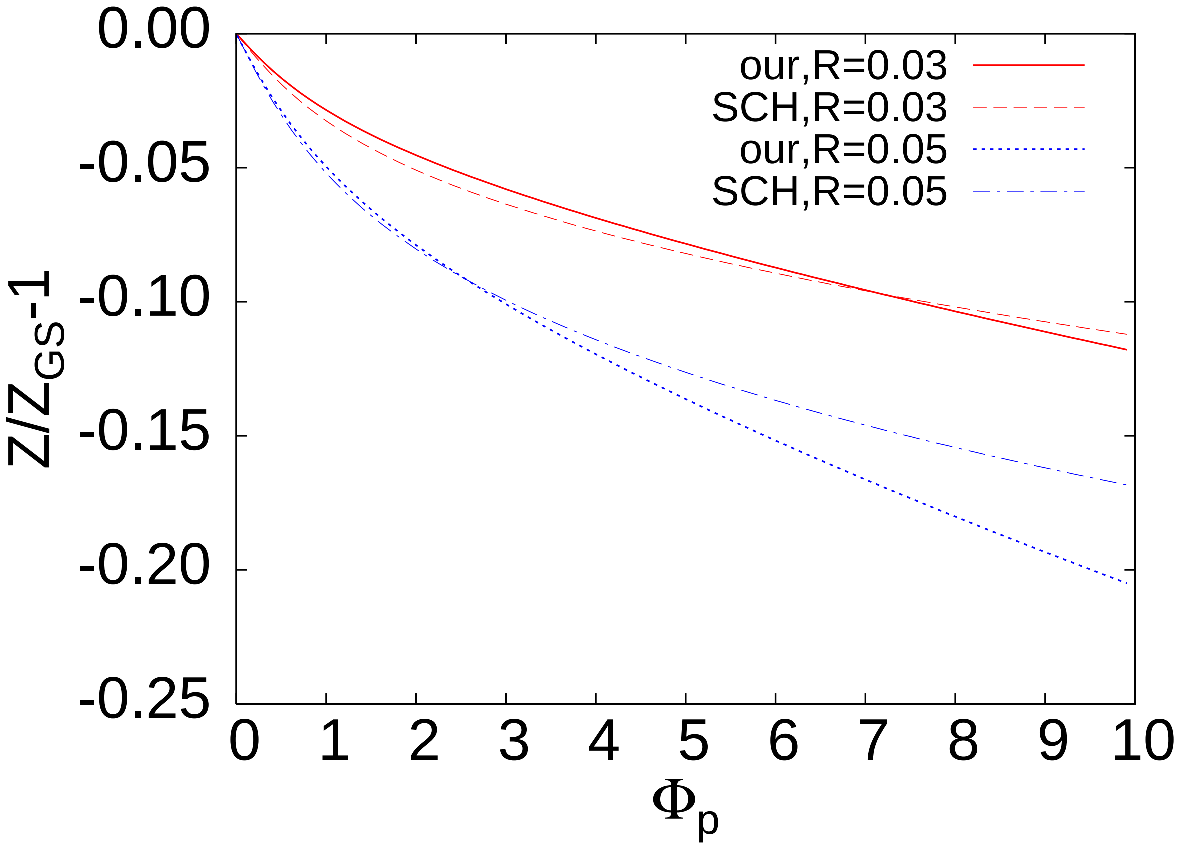

FIG. 10: Plot of $Z/Z_{GS} - 1$ versus Φ_p. Z_{GS} is the compressibility factor in the good-solvent regime, while Z corresponds to solutions with two different values of $R \equiv 1 - \Psi/\Psi^*$. We report the result (4.24) ("our") and the field-theoretical one reported in Ref.[5] ("SCH").

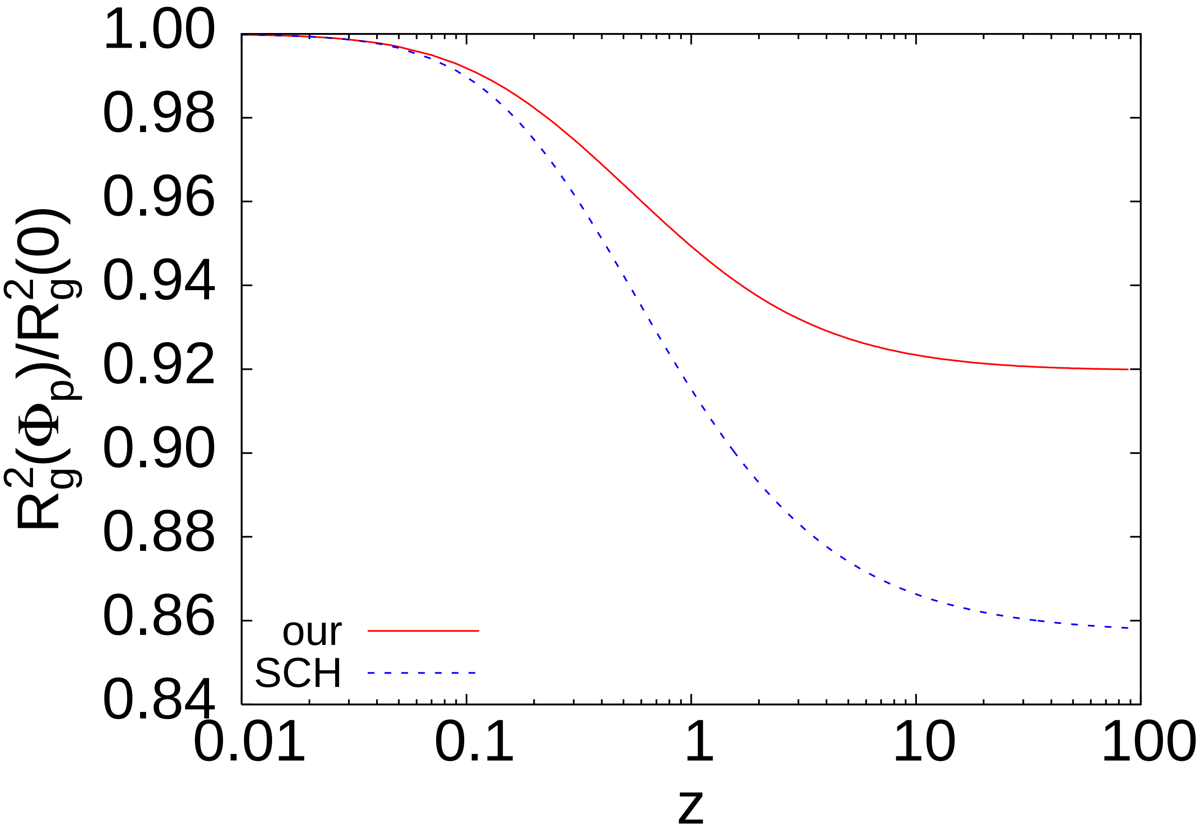

FIG. 11: The ratio $R_g^2/\hat{R}_g^2$ at $\Phi_p = 1$ as a function of z. We report our results ("our") and the field-theoretical ones reported in Ref.[5] ("SCH").

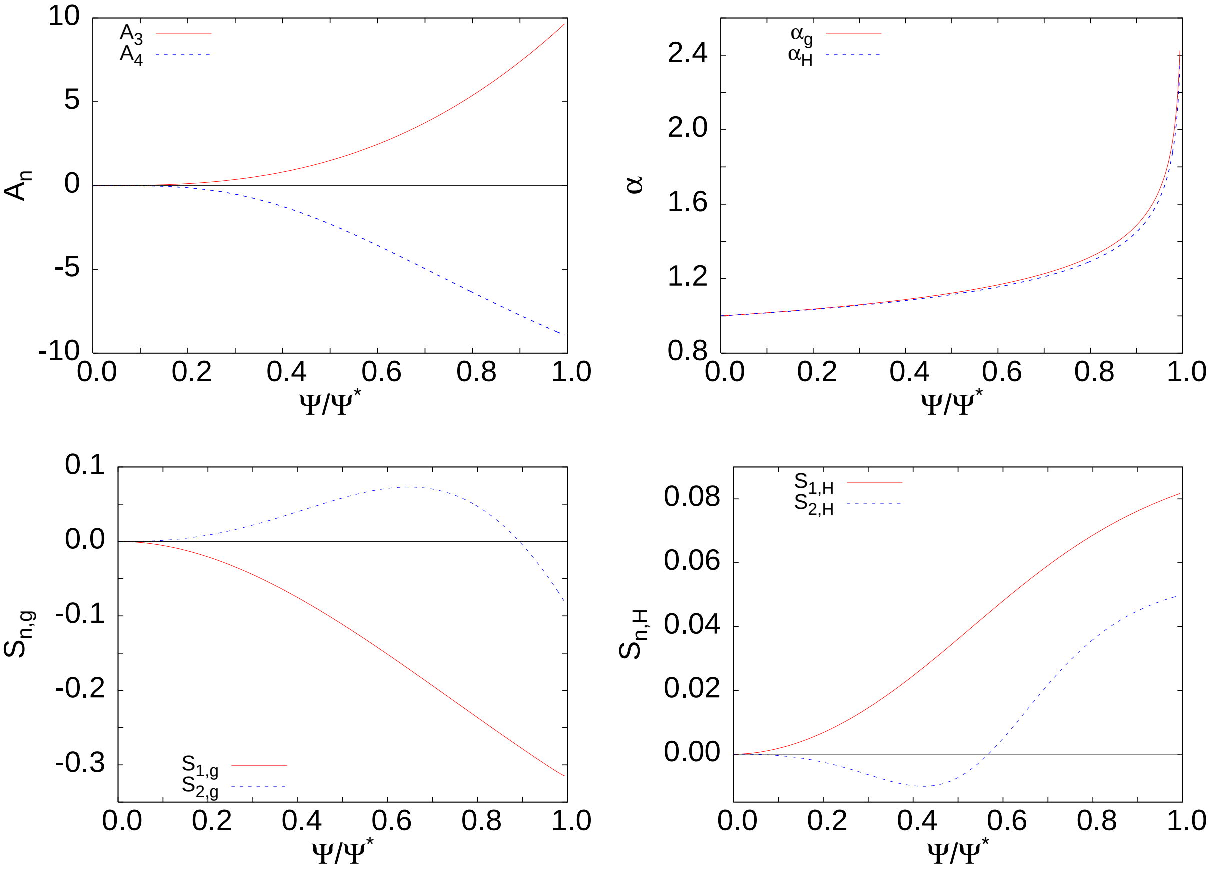

FIG. 12: The crossover functions vs Ψ/Ψ^*. We report: (top left) A_3 and A_4; (top right) α_g and α_H; (bottom left) $S_{1,g}$ and $S_{2,g}$; (bottom right) $S_{1,H}$ and $S_{2,H}$.